Electronic Supplementary Information

Cyclometalated platinum(II) complexes of 2,2'-bipyridine *N*-oxide containing 1,1'-bis(diphenylphosphino)ferrocene ligand: Structural, computational and electrochemical studies

Hamid R. Shahsavari,[a] Masood Fereidoonnezhad,[b,e*] Maryam Niazi,[a] S. Talaat Mosavi,[a] Sayed Habib Kazemi,[a] Reza Kia,[c]* Shima Shirkhan,[b] Siamak Abdollahi Aghdam[a] and Paul R. Raithby[d]*

[a]Department of Chemistry, Institute for Advanced Studies in Basic Sciences (IASBS), Yousef Sobouti Blvd., Zanjan 45137-6731, Iran.

[b]Department of Medicinal Chemistry, School of Pharmacy, Ahvaz Jundishapur University of Medical Sciences, Ahvaz, Iran.

[c]Chemistry Department, Sharif University of Technology, P.O. Box 11155-3516, Tehran, Iran.

[d]Department of Chemistry, University of Bath, Claverton Down, Bath, Avon BA2 7AY, United Kingdom.

[e]Cancer, Environmental and Petroleum Pollutants Research Center, Ahvaz Jundishapur University of Medical Sciences, Ahvaz, Iran.

Email: shahsavari@iasbs.ac.ir; fereidoonnezhad-m@ajums.ac.ir, rkia@sharif.edu

Contents:	**Page**
Figure S1. ^{1}H NMR spectrum of complex **1** in $CDCl_3$ at room temperature.	3
Figure S2. ^{31}P $\{^{1}H\}$ NMR spectrum of complex **1** in $CDCl_3$ at room temperature.	4
Figure S3. ^{195}Pt $\{^{1}H\}$ NMR spectrum of complex **1** in $CDCl_3$ at room temperature.	5
Figure S4. ^{1}H NMR spectrum of complex **2** in $CDCl_3$ at room temperature.	6
Figure S5. ^{195}Pt $\{^{1}H\}$ NMR spectrum of complex **2** in $CDCl_3$ at room temperature.	7
Table S1. Crystallographic and structure refinement data for complex **2**.	8
Table S2. Absorption data in CH_2Cl_2 solution (5×10^{-5} M) at 298 K.	9
Table S3. G09/B3LYP calculated one-electron energy and percentage composition of selected frontier MOs of complex **2** expressed in terms of component fragments.	9
Figure S6. Contour plots of the selected frontier molecular orbitals of complex **2**.	10
Figure S7. Experimental and simulated UV-vis spectra for complexes **2** (calculated absorption spectra, showing by bars).	10
Table S4. Oxidation/reduction potentials for the free dppf ligand and complexes **1-4**, in acetonitrile.	11
Figure S8. Voltammograms recorded for the free dppf ligand and complexes **1-4**, in 0.05 M $LiClO_4$-Acetonitrile at a scan rate of 5 mV s^{-1}.	11

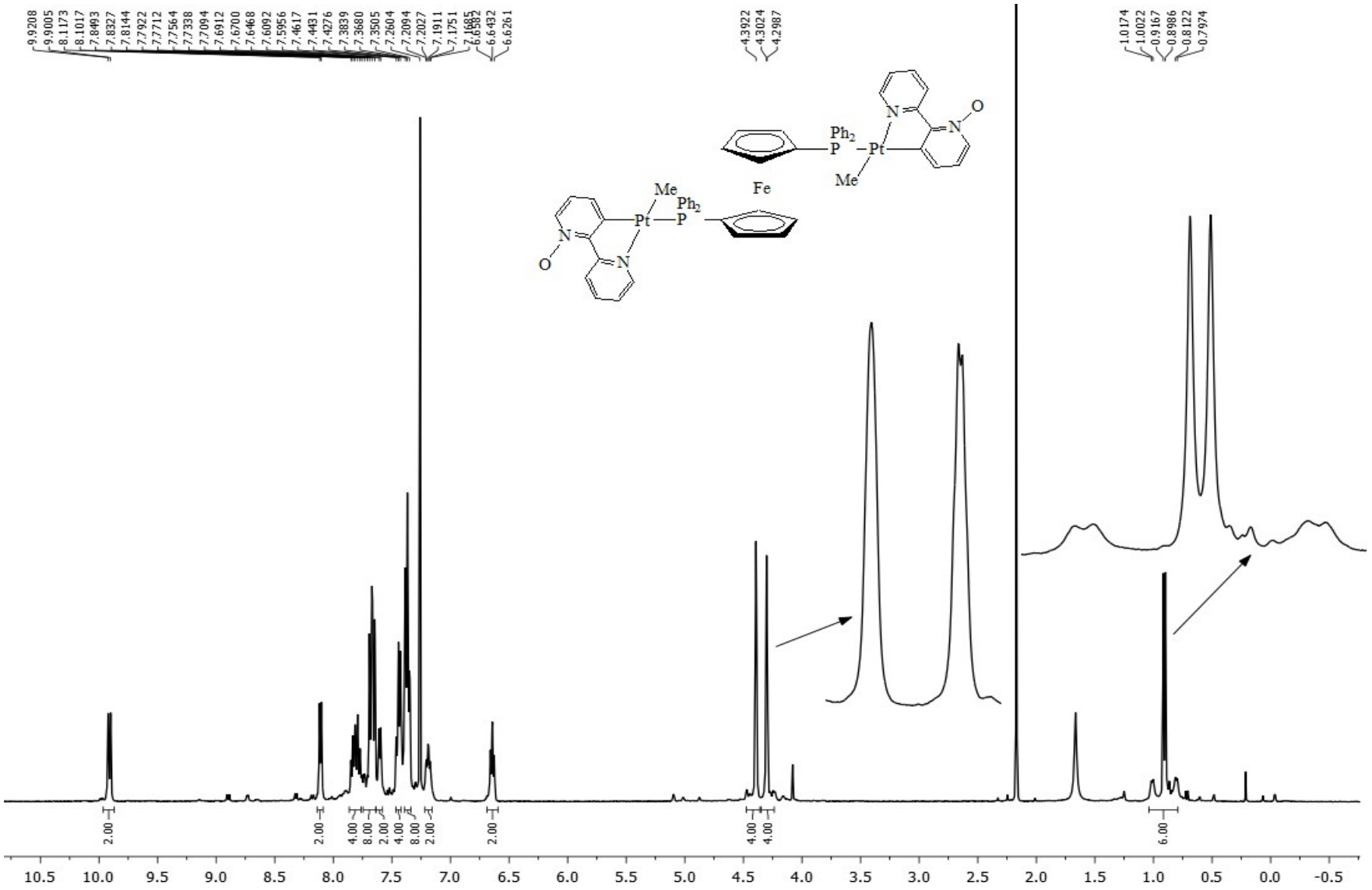

Figure S1. ^{1}H NMR spectrum of complex **1** in $CDCl_3$ at room temperature.

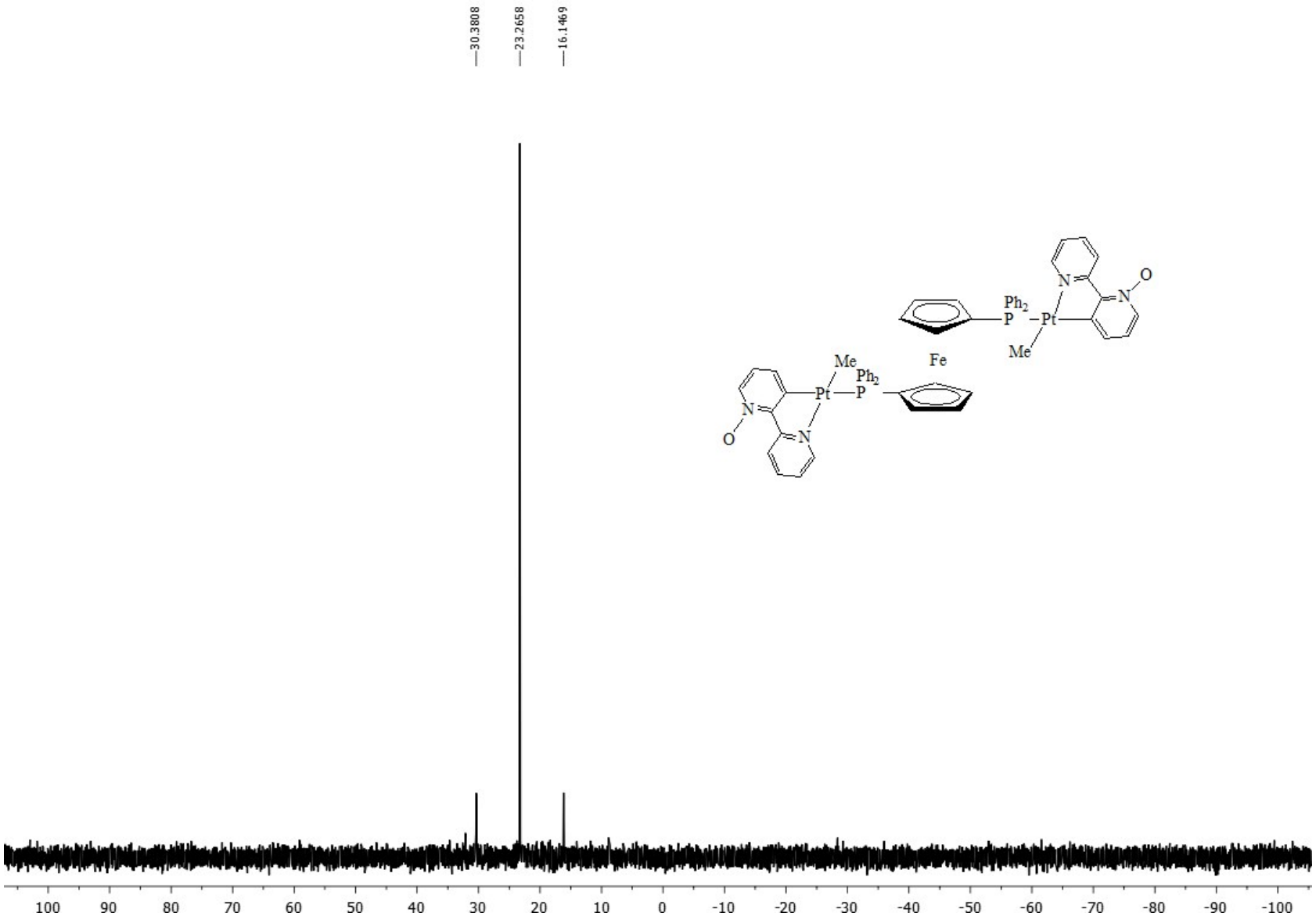

Figure S2. ^{31}P $\{^{1}H\}$ NMR spectrum of complex **1** in $CDCl_3$ at room temperature.

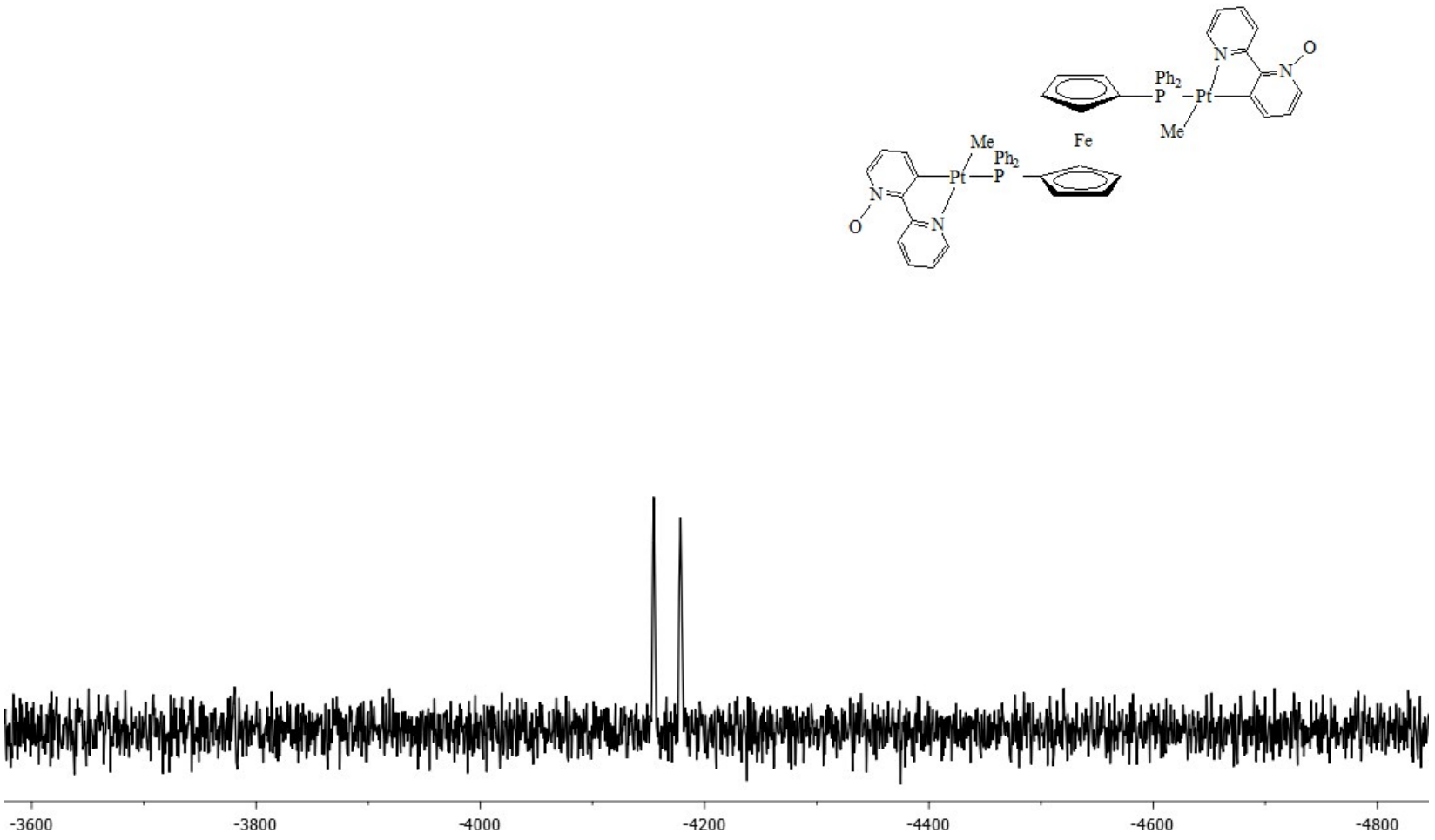

Figure S3. ^{195}Pt $\{^{1}H\}$ NMR spectrum of complex **1** in $CDCl_3$ at room temperature.

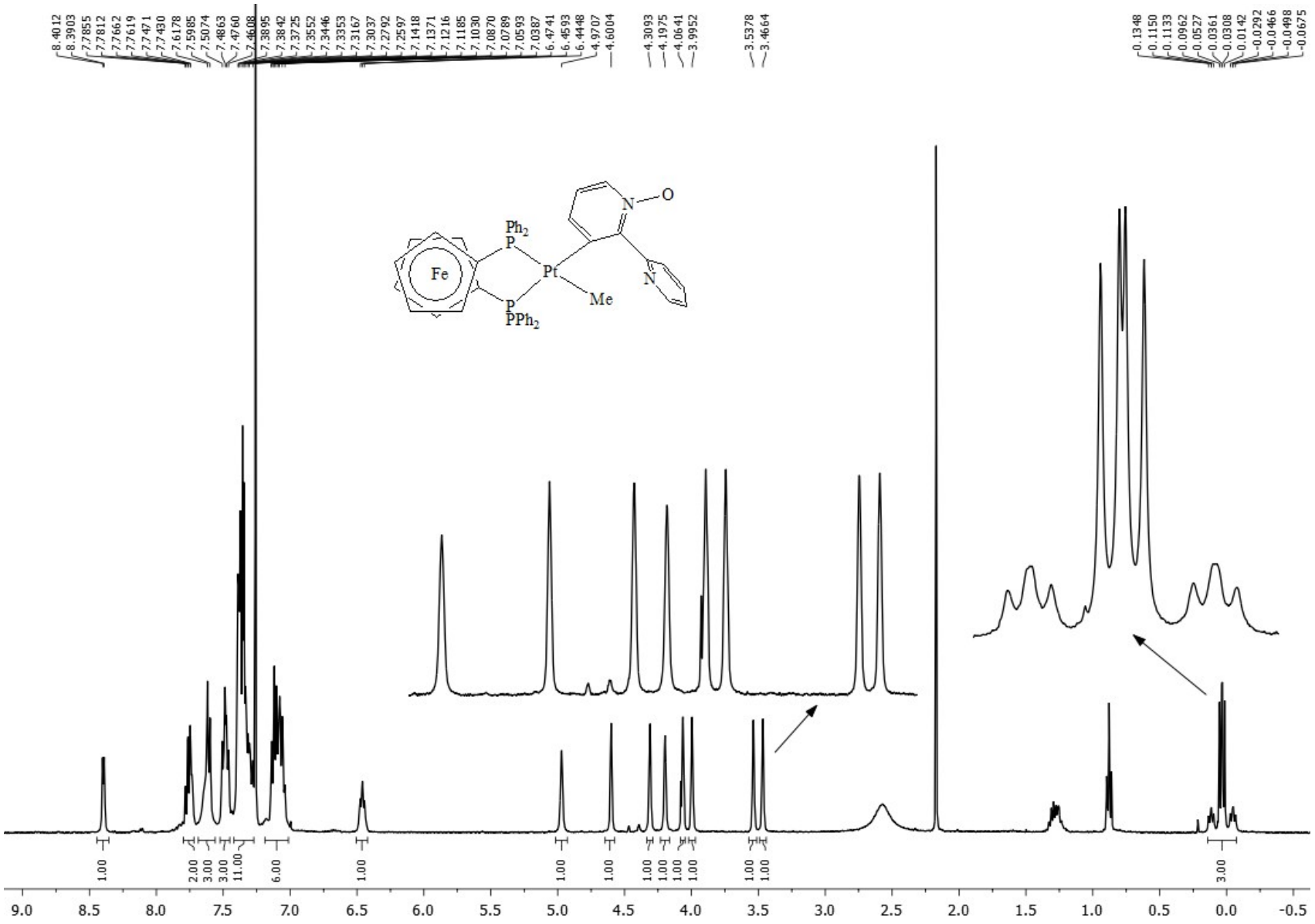

Figure S4. ^{1}H NMR spectrum of complex **2** in $CDCl_3$ at room temperature.

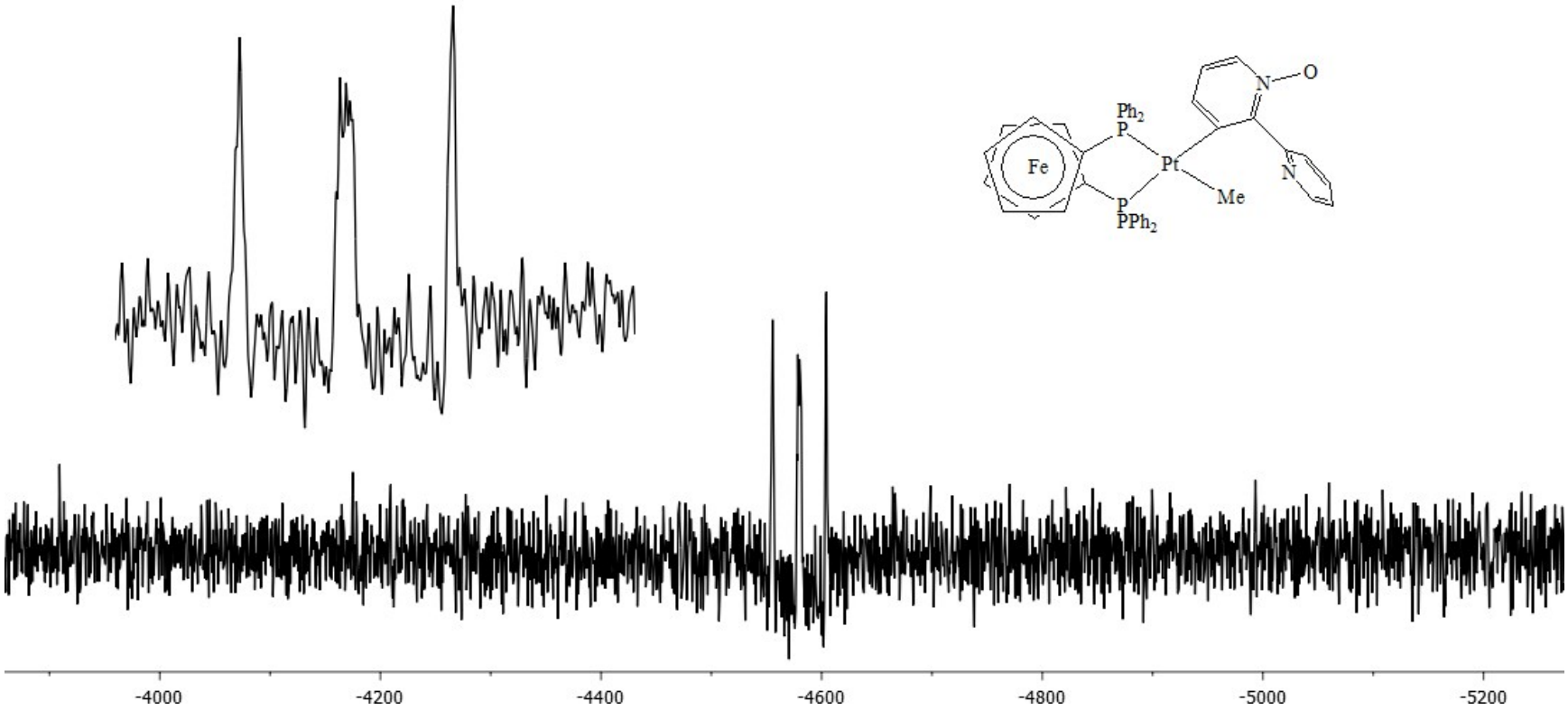

Figure S5. ^{195}Pt $\{^{1}H\}$ NMR spectrum of complex **2** in $CDCl_3$ at room temperature.

Table S1. Crystallographic and structure refinement data for complex **2**.

Formula	$C_{45}H_{38}FeN_2OP_2Pt$
Formula weight	935.65
T (K)	293(2)
λ (Å)	0.71073
Crystal system	Orthorhombic
Space Group	$P2_12_12_1$
Crystal size(mm)	0.600 × 0.200 × 0.080
a (Å)	10.49700(10)
b (Å)	11.74800(10)
c (Å)	30.0430(4)
α (°)	90
β (°)	90
γ (°)	90
V (Å^3)	3704.87(7)
Z	4
D_{calc} (g cm^{-1})	1.677
θ_{min}, θ_{max} (°)	2.934-27.450
F_{000}	1856
μ (mm^{-1})	4.289
Index ranges	-13 ≤ h ≤13
	-15 ≤ k ≤ 15
	-38 ≤ l ≤ 38
Data collected	8452
Unique data	5090
R_1[a], wR_2[b] (I > 2σ (I))	0.0466, 0.0927
R_1[a], wR_2[b] (all data)	0.0727, 0.1033
GOF on F^2 (S)	1.040
CCDC number	1511315

[a]$R_1 = \Sigma||F_o|-|F_c||/\Sigma|F_o|$, [b]$wR_2 = [\Sigma(w(F_o^5-F_c^2)^2)/\Sigma w(F_o^2)^2]^{1/2}$

Table S2. Absorption data in CH_2Cl_2 solution (5×10^{-5} M) at 298 K.

Compound	**λ_{abs}/nm (10^3 ε $M^{-1}cm^{-1}$)**
A	283 (32.1), 317_{sh} (16.4) 361 (9.2), 388 (8.6)
1	246 (40.3), 294 (27.9), 367 (8.1), 409 (5.7)
2	248 (37.4), 296 (26.3), 392 (6.1), 449 (3.4)
dppf	232 (47.1), 251 (35.6), 446 (0.48)

Table S3. G09/B3LYP calculated one-electron energy and percentage composition of selected frontier MOs of complex **2** expressed in terms of component fragments.

MO	**Character**	E (eV)	Pt	Me	bpyO-H	dppf
L + 5	dppf	-0.44	12	0.5	1.2	86.4
L + 4	dppf	-0.55	6.1	1.1	13.5	79.2
L + 3	dppf	-0.58	10.2	0.3	7.3	82.2
L + 2	bpyO-H + dppf	-0.62	17	0.4	44.7	37.9
L + 1	dppf	-0.72	2.7	0.1	3.8	93.4
LUMO	**dppf**	**-0.88**	**8.5**	**0.4**	**1.3**	**89.8**
HOMO	**bpyO-H**	**-4.82**	**4**	**0.4**	**92.8**	**2.8**
H – 1	Pt + bpyO-H	-5.40	49.5	3.3	39.9	7.2
H – 2	Pt + bpyO-H	-5.64	30.3	4.4	51.1	14.2
H – 3	dppf	-5.76	2.8	0.2	8.5	88.5
H – 4	dppf	-5.77	0.8	0.1	0.7	98.4
H – 5	bpyO-H	-5.86	17.9	4.4	60.6	17.1

Energy gap (ΔE) = **3.94 eV** (HOMO-LUMO).

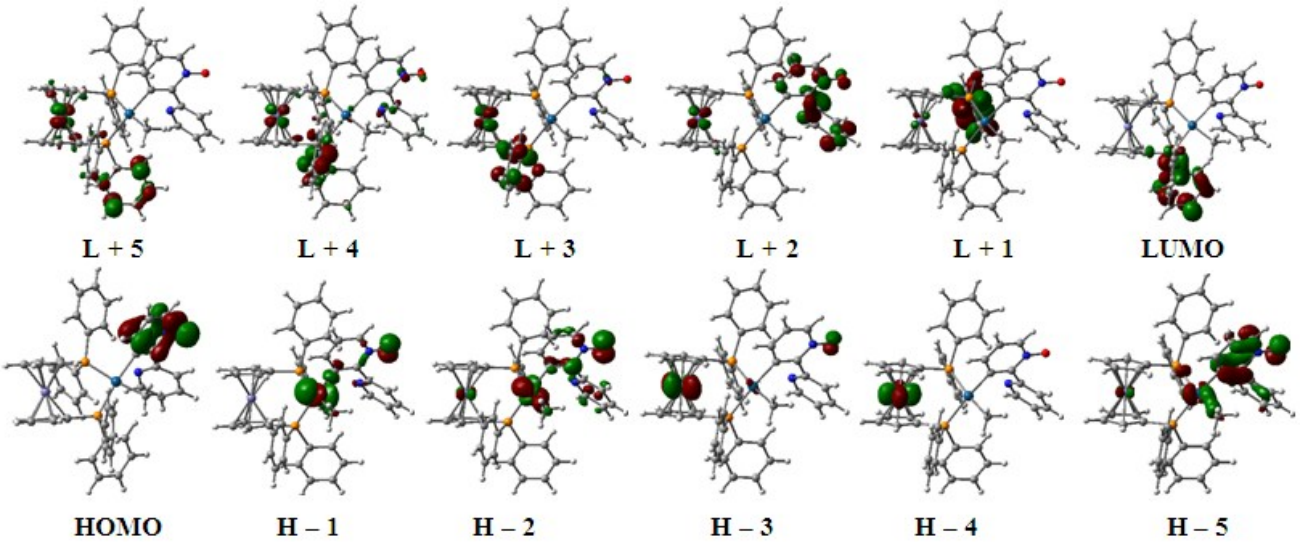

Figure S6. Contour plots of the selected frontier molecular orbitals of complex **2**.

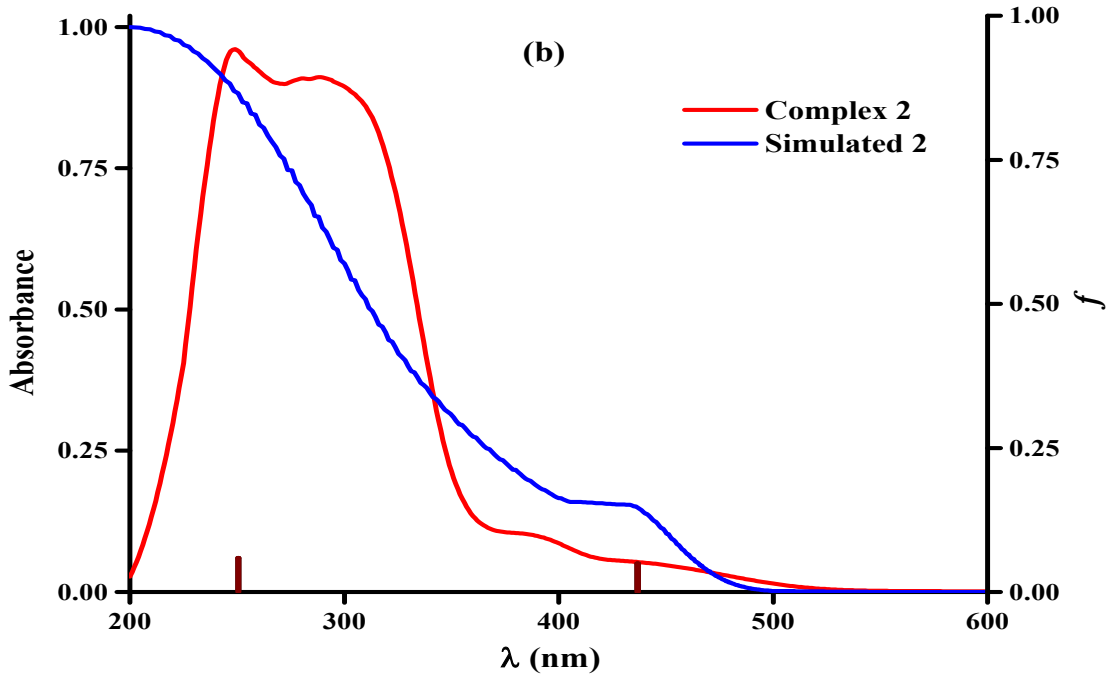

Figure S7. Experimental and simulated UV-vis spectra for complexes **2** (calculated absorption spectra, showing by bars).

Table S4. Oxidation/reduction potentials for the free dppf ligand and complexes **1-4**, in acetonitrile.[a]

Compound	E_p^{red} / V	E_p^{ox} / V
1	-0.68	+0.07,+0.27 and +1.45
2	ND[b]	+1.27
3	-0.64	+0.07, +0.43
4	-0.81	+1.47
dppf	ND	+1.25

[a] All measurements were carried out at 298 K with 0.05 M $LiClO_4$-Acetonitrile. Scan rate is 5 mV s^{-1} and versus Ag/AgCl reference electrode.

[b] Not determined (no sharp peaks found).

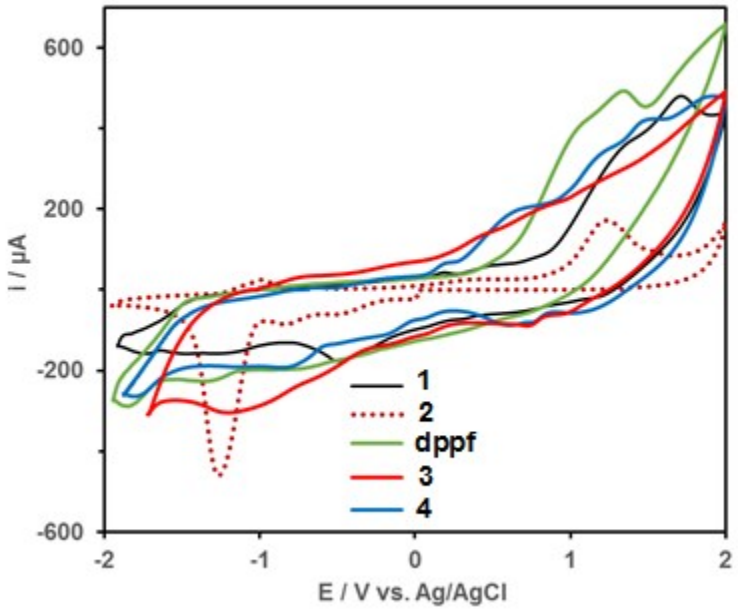

Figure S8. Voltammograms recorded for the free dppf ligand and complexes **1-4**, in 0.05 M $LiClO_4$-Acetonitrile at a scan rate of 5 mV s^{-1}.